NATIONAL CENTRE FOR CATALYSIS RESEARCH

INDIAN INSTITUTE OF TECHNOLOGY MADRAS

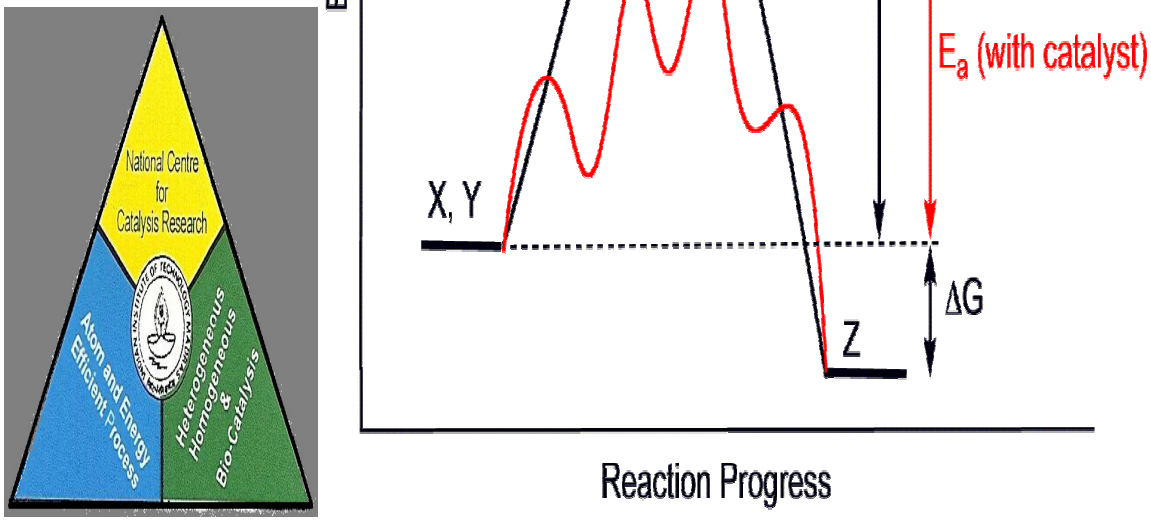

Abstracts of the

THIRD ANNUAL DAY RESEARCH SCHOLARS SEMINAR

Dated August 1, Saturday 2009

At M V C Sastri Hall of the Centre

PROGRAMME

Venue : M V C SASTRI HALL of the centre
Date 1st August 2009 (Saturday)

9.00 to 9.10 a.m.	Introduction	Preface – page 3
9.10 to 9.30 a.m.	Presentation 1	Mr.B. Kuppan - Pt/OMC for DMFC Applications- page 18
9.30 to 9.50 a.m.	Presentation 2	Dr.S.Navaladian - Synthesis of noble metal (Ag, Au, Pt and Pd) nanoparticles by oxalate-based methods – Page 20
9.50 to 10.10 a.m.	Presentation 3	Mr.S. Mahendran -Vapor phase dehydration of Glycerol over alumina -supported silico-tungstic acid catalyst- page 16
10.10 to 10.30 a.m.	Presentation 4	Ms.T.Nithya –On the changes in the crystalline nature of the support as a result of metal loding by XRD and TEM & TEM- page 10
10.30 to 11.00 a.m.	Coffee Break	Informal discussion on the centre
11.00 to 11.20 a.m.	Presentation 5	Mr.P.Indraneel – Activated carbon materials from *Calotropis Gigantea* – Page 4
11.20 to 11.40 a.m.	Presentation 6	
11.40 to 12.00 Noon	Presentation 7	T.M. Sankaranarayanan - Hydroprocessing of diesel and vegetable oil blends – page 27
12.00 to 12.20 p.m.	Presentation 8	Dr.K.Joseph Antony- Synthesis and structural studies of phosphate and sulphate modified high surface area titania – Page 14
12.20 to 12.40	Presentation 9	Mr.Anil Kumar - Terminal Oxidation of Dodecane using Microporous Alumino phosphate catalysts – page 24
12.40 to 12.50 p.m.	Presentation 10	B.Viswanathan – Some concepts on carbon dioxide Activation – Page 12
12.50 to 1.40 p.m.	LUNCH at Tifanys	

PREFACE

National Centre for Catalysis Research is a centre for academic and innovative activities in the area of catalysis, was founded in July 28, 2006 with the generous funding by the Department of Science and Technology, (DST) Government of India. The centre is established as a part of the Indian Institute of Technology, Madras. The centre has in these three years has evolved the following as its prime focus for activities.

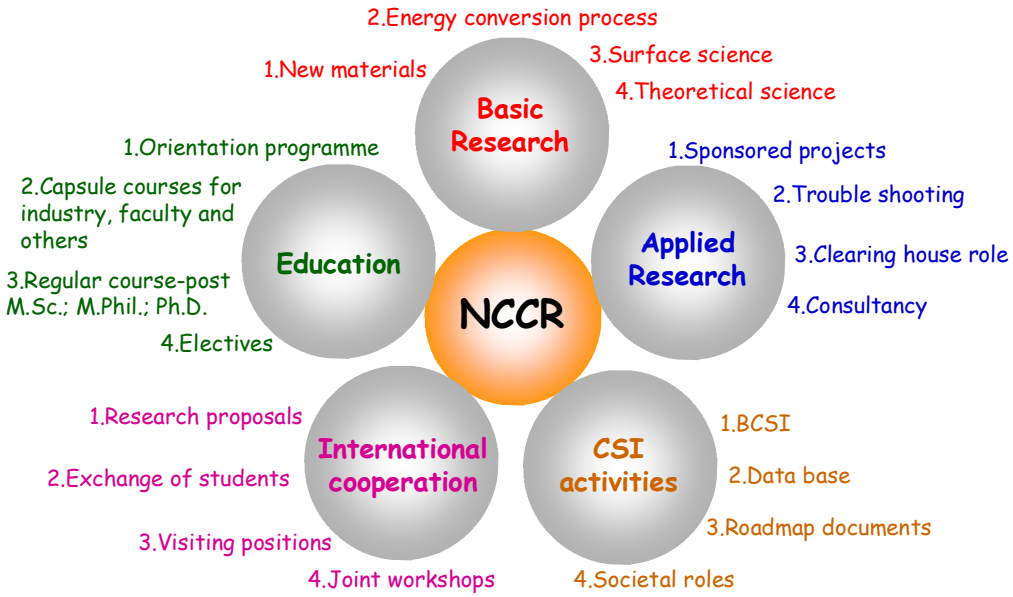

In this proposed listing of the activities the centre has been striving hard for the past three years to achieve some level of success. With the conventional limitations and shortcomings the centre has been fairly successful to achieve some level of success in each of the activities shown in this presentation above.

During these three years the centre has benefited from the constant advice of the Management and Advisory Committee chaired by Professor M M Sharma and also by the constant support and monitoring by Professor M S Ananth Director IIT M.

The centre has held all its annual days and also has started a research scholars seminar once in every six months. The centre has also been striving to bring many innovative schemes and one such is the e book series. It is hoped that the centre will become an established academic centre with the introduction of M Tech programme during the July –November 2009 session in addition to the continuing (for the 10th time) the orientation programme in catalysis conducted annually for the research scholars of this country. We do hope we will do better in the coming years.

ACTIVATED CARBON MATERIALS FROM CALOTROPIS GIGANTEA

P. Indra Neel, B. Viswanathan and T. K. Varadarajan

National Centre for Catalysis Research, Department of Chemistry,
Indian Institute of Technology Madras, Chennai 600 036

Keywords: Activation, Textural parameters, Morphology, Commercial Carbon Materials

Activated carbon materials being available in different forms like palletized, granular, powdered or molded with each form having its own advantage [1] (for instance, the intra particle adsorption kinetics is faster in the fiber form) have been extensively exploited for a variety of purification (water and air) and separation (adsorption of volatile organic compounds, pesticides, phenolic compounds dyes and metal ions) and storage (methane, hydrogen, charge storage in super capacitors) applications [2-6].

Activated carbon materials are not just a laboratory excitement, but find invaluable technological applications. Typical advantages of the use of activated carbon materials include: High quality of the effluent achievable, simplicity of the process design and ease of operation. In addition, the carbon materials being insensitive to toxic substances and corrosive environments, the regeneration is possible and easy rendering the industrial use of activated carbon materials an economically viable option [7]. The specific physico chemical properties that make activated carbon materials a potential adsorbent for pollutants include: high specific surface area, porous architecture, high adsorption capacity and surface functionality [8].

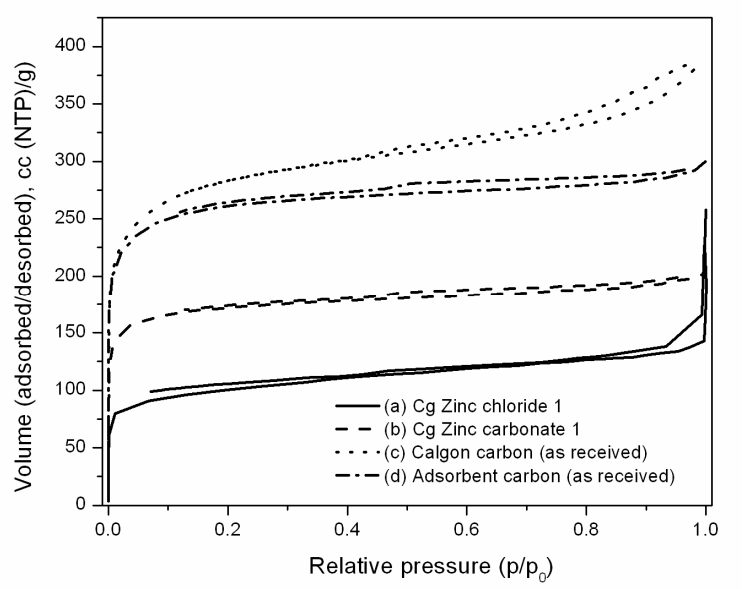

Fig. 1. N_2 adsorption-desorption isotherms of activated carbon materials (a) Cg zinc chloride 1 (S_{BET} = 356 m^2/g, Vp = 0.213 cc/g) (b) Cg zinc carbonate 1 (S_{BET} = 623 m^2/g,

Vp = 0.306 cc/g) (c) Calgon carbon (S_{BET} = 950 m^2/g, Vp = 0.451 cc/g) and (d) Adsorbent carbon (S_{BET} = 1014 m^2/g, Vp = 0.587 cc/g)

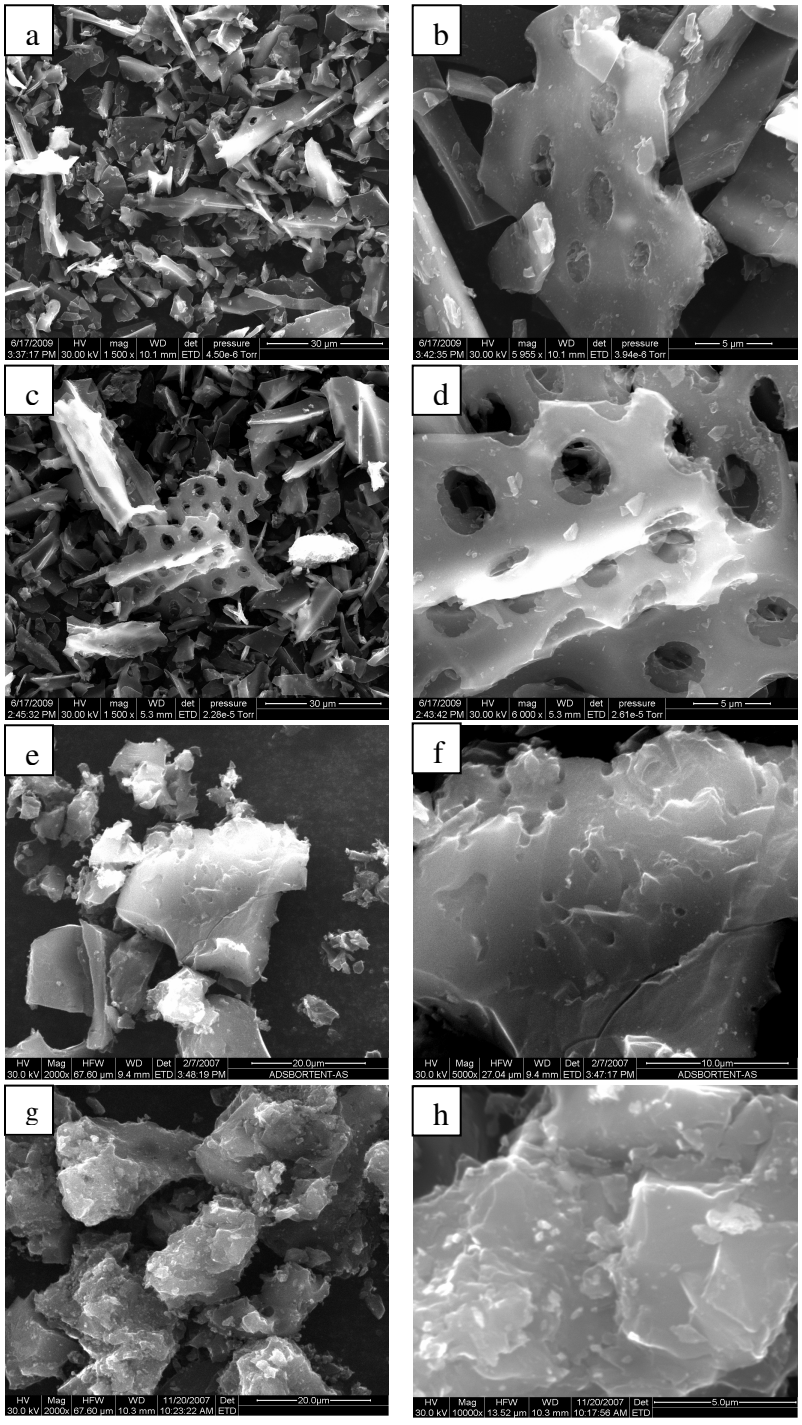

Fig. 2. SEM images of activated carbon materials at different magnifications (a) Cg zinc chloride 1, 1500 X , (b) Cg zinc chloride 1, 5,955 X, (c) Cg zinc carbonate 1, 1500 X (d) Cg zinc carbonate 1, 6000 X (e) Adsorbent carbon, 2000 X (f) Adsorbent carbon, 5000 X (g) Calgon carbon, 2000 X and (h) Calgon carbon, 10, 000 X

In the present work a novel source, Calotropis gigantea stems, has been identified as a promising carbon precursor for the production of activated carbon materials. A cluster of activating agents belonging to different classes namely, transition metal compounds ($ZnCl_2$, $ZnCO_3$), alkali metal halides (NaCl, NaBr, NaI, KBr and KI), alkali metal carbonates (Li_2CO_3, Na_2CO_3, K_2CO_3) and alkali metal salts of carboxylic acids ($Na_2C_2O_4$) were exploited to tune the structural, textural and morphological features of the resulting carbon materials [9]. Among the class of transition metal salts ($ZnCl_2$ and $ZnCO_3$), $ZnCO_3$ was found to be a better activating agent with improved specific surface area values (Fig. 1.) and well developed pore structure (Fig. 2.) compared to $ZnCl_2$. Also, both $ZnCO_3$ and $ZnCl_2$ activation processes yielded peculiar pore structure which is unique to and is characteristic of the plant source and such features are absent in the commercial carbon materials like Calgon and Adsorbent carbon materials. The intense activation with ZnCO3 is a result of the accompanied evolution of CO_2 during the decomposition of ZnCO3 which is not possible in the case of ZnCl2. Also $ZnCO_3$, being non hygroscopic offers better contact and better reactivity with char compared to ZnCl2 (hygroscopic). In addition, the formation of ZnO in the case of ZnCO3 activation is due to the direct decomposition of ZnO where as the ZnO formation is a result of the redox reaction between $ZnCl_2$ and the char resulting in the difference in the reactivity of ZnO formed in both $ZnCO_3$ and $ZnCl_2$ activation processes. Thus $ZnCO_3$ acts as better activating agent than $ZnCl_2$.

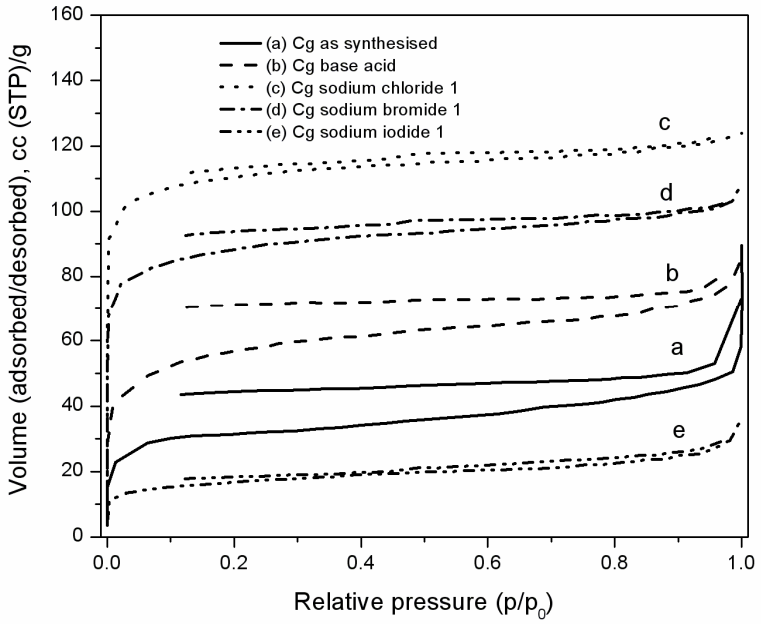

Fig. 3. N_2 adsorption – desorption isotherms of (a) Cg as synthesized (S_{BET} = 97 m^2/g, Vp = 0.08 cc/g) (b) Cg base acid (S_{BET} = 203 m^2/g, Vp = 0.12 cc/g) (c) Cg sodium chloride 1 (S_{BET} = 400 m^2/g, Vp = 0.2 cc/g) (d) Cg sodium bromide 1 (S_{BET} = 319 m^2/g, Vp = 0.16 cc/g) and (e) Cg sodium iodide 1 (S_{BET} = 58 m^2/g, Vp = 0.04 cc/g)

Among alkali metal halides (NaCl, NaBr and NaI), use of NaCl resulted in a four time enhancement in the S_{BET} (BET specific surface area value) and Vp (total pore volume) where as the use of NaI as activating agent has reduced the S_{BET} and Vp values to half the value of the original char (Fig. 3). The results are in agreement with the decreasing ionicity and increasing covalency as one goes from NaCl to NaI through NaBr. Since NaI is more covalent it adsorbs strongly on the carbon surface and also blocks the incipient narrow pores in the char preventing any further activation. More over, for the same amount (wt.) of the activating agent, the wt.% of Na in NaCl, NaBr and NaI were respectively 39.3, 22.3 and 15.3 indicating a decrease in Na content. As one of the steps of preparation of activated carbon involves treatment with conc. HCl, lowering of Na content in the activating mixture leads to poor activation of the carbon material.

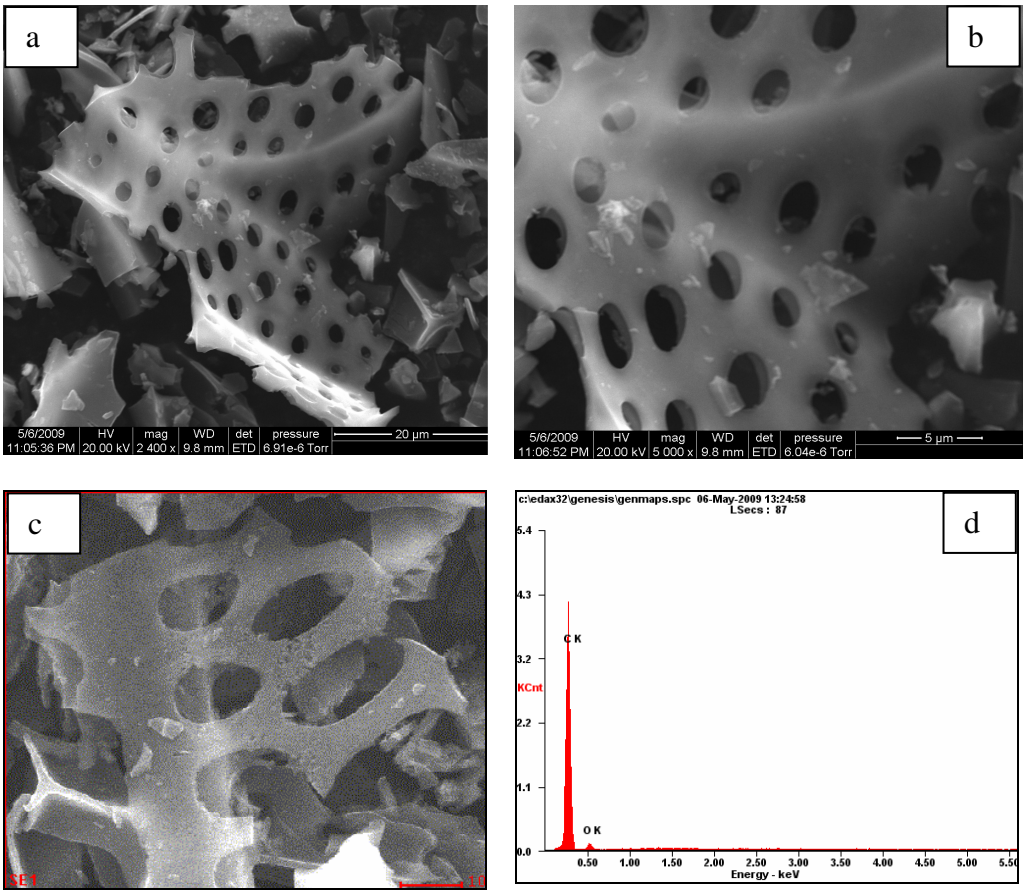

Fig. 4. FEG SEM images (at different magnifications) of activated (carbonate) carbon material from Calotropis gigantea, Cg carbonate 3, along with EDS (Energy Dispersive Spectroscopy) spectrum: (a) 2400 X, (b) 5000 X and (c & d) FEG SEM image with EDS spectrum

Under the class of alkali metal carbonates as activating agents, K_2CO_3 exhibited excellent performance as activating agent with S_{BET} value of 1296 m^2/g, a value greater than the S_{BET} values of commercial carbon materials, namely, Adsorbent carbon (S_{BET} = 1014

m^2/g), Black Pearl 2000 (S_{BET} = 1012 m^2/g), Calgon (S_{BET} = 950 m^2/g), Vulcan XC 72 R (SBET = 224 m^2/g) and CDX 975 (S_{BET} = 215 m^2/g).

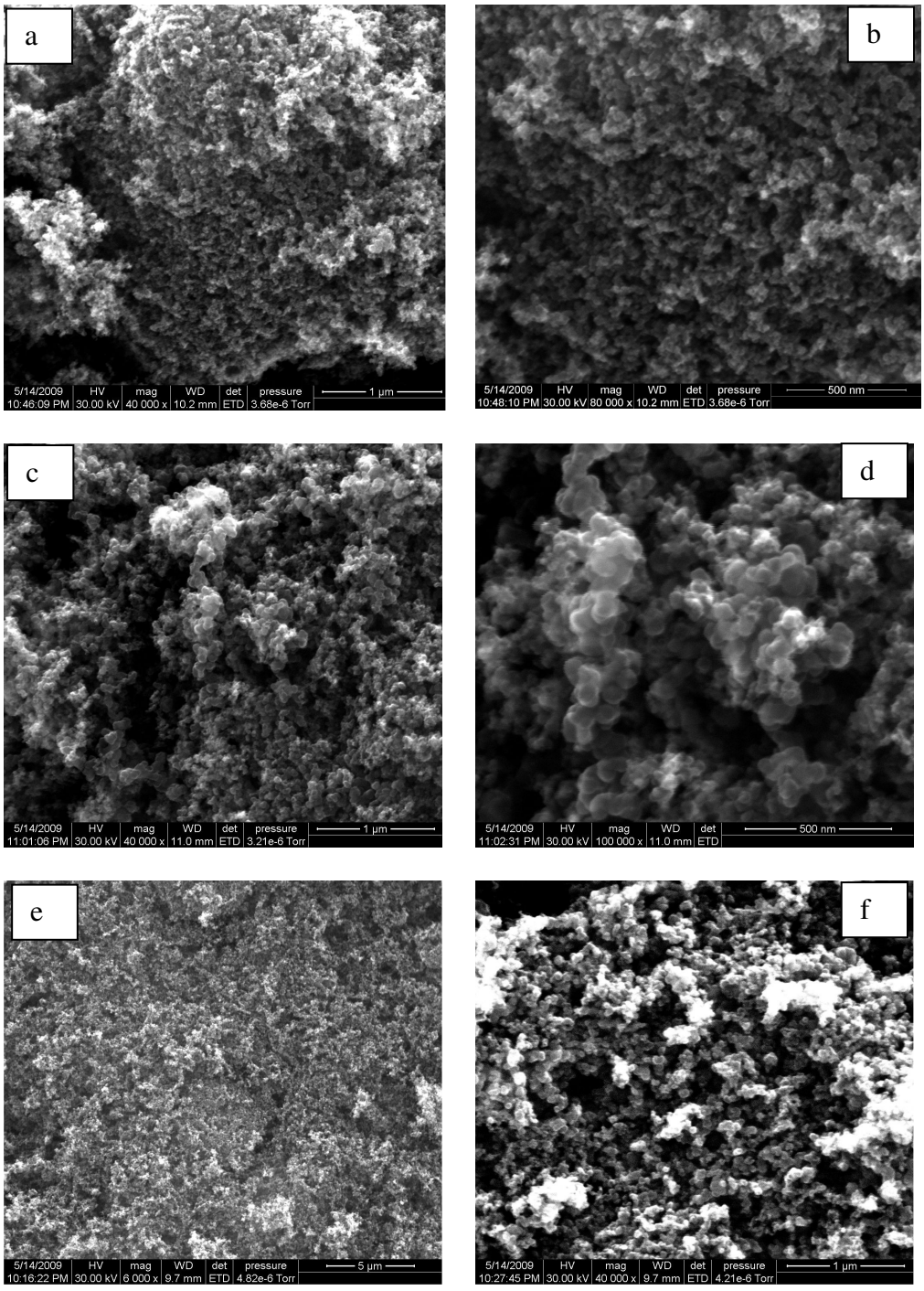

Fig. 5. FEG SEM images (at different magnifications) of commercial activated carbon material: (a & b) Black Pearl 2000 (40, 000 X, 80, 000 X), (c & d) Vulcan XC 72 R (40, 000 X, 1,00, 000 X) and (e & f) CDX 975 (6000 X, 40, 000 X)

In addition to surpassing the commercial carbon materials in terms of textural parameters, the activated carbon material from Calotropis gigantea produced by using K_2CO_3 as activating agent exhibited unique pore structure (Fig. 4.) which is not observable in any of the commercial activated carbon materials like Black Pearl 2000, Vulcan XC 72 R and CDX 975 (Fig. 5.) [10].
Thus the choice of the carbon precursor as well as the method of activation are the two crucial issues that determine the quality and the nature of the activated carbon material derivable.

References:

1 Motoyuki Suzuki, Carbon 32 (1994) 577
2 C. Brasquet and P. Le Cloirec, Carbon 35 (1997) 1307
3 P. Magne and P. L. Walker, JR, Carbon 24 (1986) 101
4 Md. Zahangir Alam, Suleyman and A. Muyibi, Journal of Environmental Sciences, 19 (2007) 103
5 T. Otowa, Y. Nojima and T. Miyazaki, Carbon 35 (1997) 1315
6 K. Kadirvelu, M. Kavipriya, C. Karthika, M. Radhika, N. Vennilamani and S. Pattabhi, Bioresource Technology, 87 (2003) 129
7 Xiaoning Wang, Nanwen Zhu and Bingkui Yin, Journal of Hazardous Materials 153 (2008) 22
8 Zoulikha Merzougui and Fatima Addoun, Desalination 222 (2008) 394
9 B. Viswanathan, P. Indra Neel and T. K. Varadarajan, Catalysis Surveys from Asia, Accepted
10 B. Viswanathan, P. Indra Neel and T. K. Varadarajan, Carbon, Under revision

ON THE CHANGES IN THE CRYSTALLINE NATURE OF THE SUPPORT AS A RESULT OF METAL LOADING BY XRD & TEM

T.Nithya, B.Viswanthan, and P.Selvam.

Key Words: Heterogeneous catalysis, X-Ray Diffraction, Support Crystallinity, Metal dispersion, Transmission Electron Microscopy, Crystallite size.

Conventionally XRD has been used to evaluate the effects on the support as result of metal loading which are employed as heterogeneous catalysts. The scientific community usually identify the metal and the support phases and changes therein by XRD at various levels of metal on to the support. In addition in a series of metal supported catalysts, the effect of support or the metal loaded on it in causing the changes in the phase composition have been studied by X-Ray diffraction and Transmission Electron Microscopy (TEM). XRD gives better information on the crystallinity of support or metal phase, dispersion of metal, also facilitate the determination of crystallite size. The crystallite size and the metal dispersion are further identified by TEM. These results suggest that metals at lower loading or high dispersion on support retains the amorphous nature of the support and their crystallite size will depends on the different calcination temperature of the catalysts. At higher loading, the metal oxide phase is formed or the intensity of the peak increased which may change the activity of catalysts. In addition the whole catalysts crystallinity depends on the different calcination temperatures adopted.

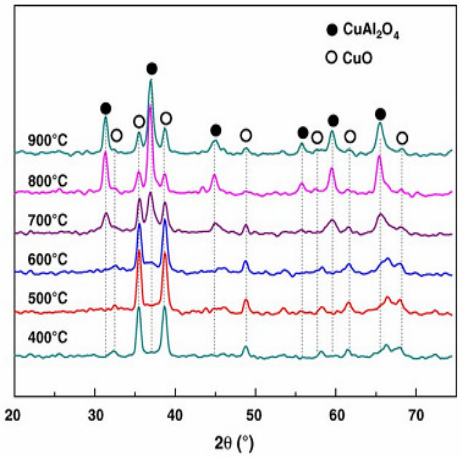

XRD patterns of CuO (33.3%)/Al_2O_3 catalysts calcined at different Temperatures

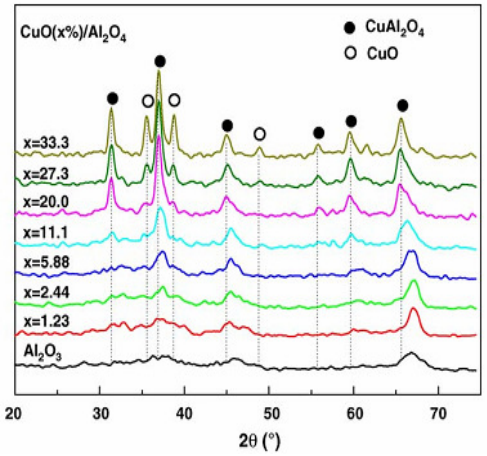

XRD patterns of CuO (x %) /Al_2O_3 catalysts calcined at 800°C.

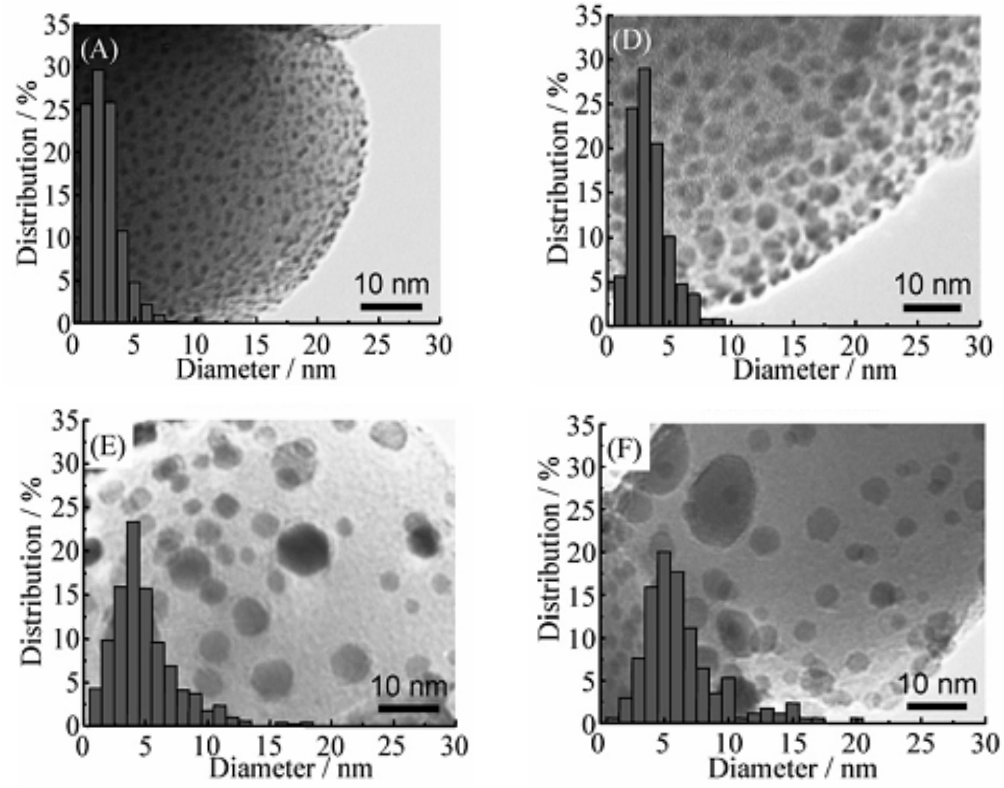

TEM images of TiO_2 supported Ru nanoparticles. (A) Ru/TiO_2(B), (D) Ru/TiO_2(B500), (E) Ru/TiO_2(B700), (F) Ru/TiO_2(B800) – $^{(B)}$As-synthesized

Table 1 . Metal dispersion and Mean particle diameter of the catalysts

Sample	Metal content [wt%]	Mean particle size (D)/nm
Ru/TiO_2(B)	0.80	2.5
Ru/TiO_2(B500)	0.80	3.4
Ru/TiO_2(B700)	0.80	5.4
Ru/TiO_2(B800)	0.80	6.0

References:

1) Meng-Fei Luo, Ping Fang, Mai He, Yun-Long Xie, **Journal of Molecular Catalysis A: Chemical, 239 (2005) 243.**

2) Takayuki Abe, Masaaki Tanizawa, Kuniaki Watanabe and Akira Taguchi, **Energy Environmental Science, 2 (2009) 315.**

CONCEPTS ON THE ACTIVATION OF CARBON DIOXIDE

B.Viswanathan

It has been a challenging proposition for catalyst community to deal with the activation of typical molecules like CO, N_2 and CO_2 whose HOMO levels are not bonding orbitals In the case of carbon dioxide the partial molecular orbital scheme leaving out the core levels can be represented as $(1\sigma_g)^2$ $(1\sigma_u)^2$ $(2\sigma_g)^2$ $(2\sigma_u)^2$ $(1\pi_u)^4$ $(1\pi_g)^4$ …. In this, the bonding orbitals are $(1\sigma_g)^2$ $(1\sigma_u)^2$ and $(1\pi_u)^4$ while the non bonding orbitals are $(2\sigma_g)^2$ $(2\sigma_u)^2$ and $(1\pi_g)^4$. Even though many modes of activation of such molecules have been proposed, still there is no way to selectively activate the molecule and convert them to useful chemicals. This situation is particularly applicable for carbon dioxide since any activation will be reflected on both sides of the molecule and hence preferential conversion is not realized. Chemical reactivity is normally seen in the oxidation/reduction or removal/addition of electrons. The charge transfer is normally encountered in various modes of activation and in the case of carbon dioxide also one can utilize various modes of activation like chemical activation, electrochemical activation and photochemical activation.

Scheme 1. Various modes of activation of carbon dioxide

- **Radiochemical: $CO_2 \xrightarrow{\gamma\text{-radiation}} HCOOH, HCHO$**
- **Chemical reduction $2Mg + CO_2 \rightarrow 2MgO + C$**
  $Sn + 2CO_2 \rightarrow SnO_2 + 2CO$
  $2Na + 2CO_2 \rightarrow Na_2C_2O_4$
- **Thermo chemical $CO_2 \xrightarrow{Ce^{4+}} CO + ½O_2$; (T>900 °C)**
- **Photo chemical $CO_2 \xrightarrow{h\nu}$ CO, HCHO, HCOOH**
- **Electrochemical $CO_2 + xe^- + xH^+ \rightarrow$ CO, HCOOH, $(COOH)_2$**
- **Biochemical $CO_2 + 4H_2 \xrightarrow{\text{bacteria}} CH_4 + 2H_2O$**
- **Biophotochemical CO_2 + oxoglutaric acid $\xrightarrow{h\nu}$ isocitric acid**
- **Photo electrochemical $CO_2 + 2e^- + 2H^+ \xrightarrow{h\nu} CO + H_2O$**
- **Bioelectrochemical CO_2 + oxoglutaric acid $\xrightarrow{\text{enzyme}}$ isocitric acid methylviologen**
- **Biophotoelectrochemical $CO_2 \xrightarrow{h\nu.\ \text{enzyme, p-1nP}} HCOOH$ eV, methylviologen**

The various possibilities in the case of carbon monoxide activation are given in scheme 1. Direct ionization (I.P. 13.78 eV and electron affinity -0.6 eV) of carbon dioxide appears to be (in the case of inert gases I.P. varies between 10.74 to 24.57 eV and the electron affinity varies between -0.2 to -0.45 eV) comparable to that of the inert gases and hence activation of carbon dioxide may be similar to the activation of inert gases. Given this situation, a second point is that activation of carbon monoxide has to be aimed at activating the carbon centre in order to generate useful chemicals. The energies of 2s and 2p orbitals of carbon are -19.4 and -10.7 eV while that of oxygen are -32.4 and -15.9 eV. This means that the 2s level of oxygen may not effectively participate in the bonding and hence the bonding levels come from the overlap of 2s and 2p orbitals of carbon with the 2p orbitals of oxygen. As stated above, the bonding orbitals are $(1\sigma_g)^2$ $(1\sigma_u)^2$ and $(1\pi_u)^4$ and the energy values are -14, and around -38 eV and thus it is seen that the bonding orbitals are stabilized compared to the original carbon orbitals. Since the HOMO is a nonbonding π orbital the optical activation (requiring nearly 10 eV) can not be very specific activating the carbon centre of the molecule. Since direct optical activation is difficult, one has to resort to charge transfer phenomenon known in semiconductor catalysis. This imposes limitations on the position of the conduction band of the semiconductor so as to facilitate smooth charge transfer from excited semiconductor to the carbon dioxide molecule. However, electro-chemical activation can be expected not only perturb the energy positions of these molecular orbitals and the electric field present near the electrode/electrolyte interface may favour orbital overlap between the substrate molecule and the electrode surface which means the orbitals of the electrode have to have suitable symmetry and energy with that of the perturbed orbitals of carbon dioxide molecule. Since 'σ' bonding orbitals of CO_2 deep down (-38 eV), it is deduced that only the π orbitals of CO_2 alone may be perturbed and hence attack on the oxygen centres alone may be possible. It appears therefore that electrochemical activation of CO_2 may be possible even compared to direct photochemical activation, thought it may be still be possible by charge transfer route. The presentation therefore, focuses on the implications of these postulates.

SYNTHESIS AND STRUCTURAL STUDIES OF PHOSPHATE AND SULPHATE MODIFIED HIGH SURFACE AREA TITANIA

K. Joseph Antony Raj and B. Viswanathan*

National Centre for Catalysis Research, Indian Institute of technology-Madras, Chennai 600036. email: bvnathan@iitm.ac.in

Abstract

The single-step organic free process was evolved in precipitating phosphate modified titania from titanium oxysulphate solution at a temperature of about 98 ^{o}C using a seed and with the addition of NaOH. The adsorption of phosphate ions from aqueous solution onto titania has been studied by XRD, XRF, XPS, DRIFT spectra, and nitrogen adsorption-desorption measurements showed the strong adsorption of phosphate on the surface of titania. The incorporation of phosphorus in the titania framework was found to inhibit the crystallization and particle growth, and was found to enhance the thermal stability due to the formation of titanyl phosphate. The phosphate modified titania material dried at 100 ^{o}C showed a surface area of 340 m^2/g which subsequently lowered to 70 m^2/g after calcination at 900 ^{o}C thus showing the thermal stability of the material, an essential property required for the application as catalyst and active support. The calcination at 900 ^{o}C for 4 hours led to the formation of stable titanium pyrophosphate which controlled the crystallinity of the material. The esterification reaction performed on P-TiO$_2$ samples showed the significance of optimum quantity of *anatase* phase and phosphate content for the catalytic activity.

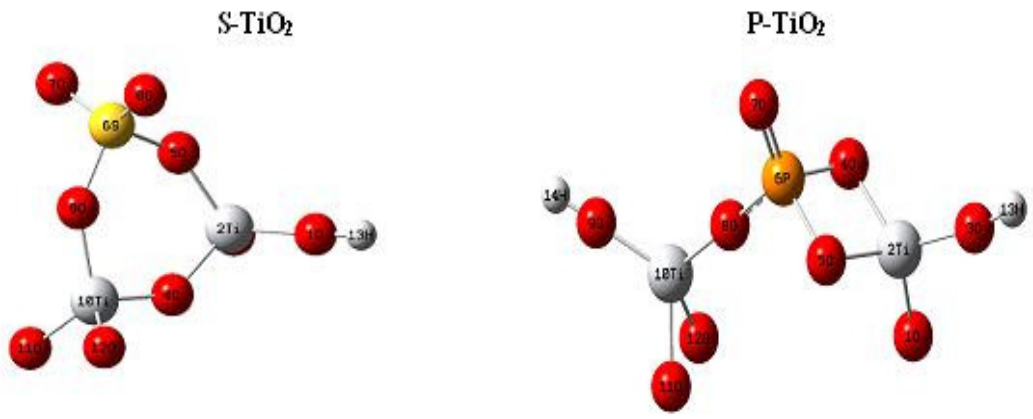

A single-step synthesis of mesoporous sulphated titania is described by seeding method using titanium oxysulphate as the titania source. The hydrolysis process is similar to the one mentioned for the synthesis of phosphate modified titania except that the phosphoric acid was excluded. The XPS and DRIFT spectra show the existence of bridged bidentate sulphate complex on the surface of titania. The elimination of sulphur on heat treatment showed a characteristic change in mesoporosity, specific surface area and crystallinity of the material. The transformation of sulphated titania to *anatase* was incomplete at 900 ^{o}C showing a delay in crystallization due to the presence of sulphate. The studies on temperature treatment of the sulphated titania showed that the material obtained can be used for various applications at temperatures below 300 ^{o}C.

References:

1. **K. Joseph Antony Raj, A.V. Ramaswamy and B. Viswanathan, J Phy. Chem. C. (Accepted)**
2. **K. Joseph Antony Raj, and B. Viswanathan, Single-step synthesis and structural study of mesoporous sulphated titania nanopowder by controlled hydrolysis process (Communicated)**

Vapor phase dehydration of Glycerol over alumina - supported silicotungstic acid catalyst

S. Mahendran, B.Viswanathan and P. Selvam*

National centre for catalysis Research, Department of Chemistry,

Indian Institute of Technology-Madras, Chennai-36, India

Key words: Glycerol, Dehydration, Acrolein, Silicotungstic acid and alumina

Dehydration of glycerol to produce Acrolein was performed over several solid acids. Supported heteropolyacids were effective as catalyst for the dehydration of glycerol. The alumina-supported catalysts were prepared by impregnation method. The catalysts were characterized by nitrogen adsorption, XRD, TG-DTA and FT-IR. The XRD pattern shows that alumina-supported catalysts were amorphous. The catalytic activity depended on extent of loading of silicotungstic acid and pore size of the alumina support. The 20 wt% silicotungstic acid supported on alumina showed the highest catalytic activity with maximum Acrolein selectivity (<50%).

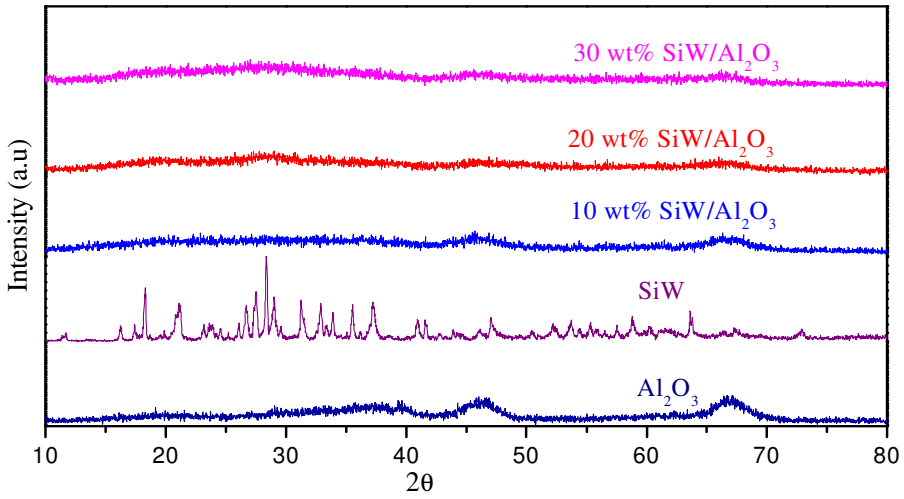

Fig . X-Ray Diffractograms for alumina supported silicotungstic catalysts

Reference:

1. Eriko Tsukuda, Satohi Sato, Ryoji Takahashi, Toshiaki Sodesawa, ***Catal.Comun.*** (2007) 1349.

2. Song-Hai Chai, Hao-Peng Wang, Yu Liang, Bo-Qing., ***J.Catal.*** 250(2007) 342

3. Hanan Atia, Udo Armbruster, Andreas Martin***, J.Catal.*** 258 (2008) 72

*** E-Mail: selvam@iitm.ac.in; bvnathan@iitm.ac.in**

ORDERED MESOPOROUS CARBON SUPPORTED PLATINUM (Pt/OMC) ELECTROCATALYST FOR METHANOL OXIDATION

B. Kuppan, B. Viswanathan and P. Selvam

National Centre for Catalysis Research, Department of Chemistry,
Indian Institute of Technology-Madras, Chennai 600 036

The PVP based ordered mesoporous carbon is prepared using polyvinyl pyrrolidone as carbon source and SBA-15 as hard silica template.[1, 2]

In this study, 20 wt. % Pt was loaded on OMC (PVP) using H_2PtCl_6. The loaded sample was then ultrasonicated for 30 min. 25 ml solution containing 30 mg $NaBH_4$ was added dropwise to the carbon suspension with stirring at room temperature. Stirring was continued for 6 h. The sample was filtered, washed with distilled water, and dried in a vacuum oven at 358 K for 12 h. The catalyst thus obtained is denoted as Pt/OMC (PVP).[3]

The catalyst was characterized by using X-ray diffraction (XRD), X-ray photoelectron spectroscopy (XPS), Scanning Electron Microscopy (SEM) and Transmission Electron Microscopy (TEM).

The electrochemical oxidation of methanol over Pt/OMC (PVP) was studied by cyclic voltammetry at room temperature. The working electrode was fabricated using 20 mg Pt/OMC (PVP) by dispersing in 0.5 ml water under ultrasonication for 20 min. A part (10 µl) of the suspension was then coated on glassy carbon (GC) electrode and dried at 348 K. Finally, 5 µl of 5 wt% Nafion was coated so as to anchor the catalyst onto the GC electrode and then dried at room temperature. [4]

Electrochemical measurement performed in 1 M H_2SO_4 + 1 M CH_3OH indicate the as-prepared Pt/OMC(PVP) catalyst exhibit good activity for methanol oxidation and it is comparable with the other mesoporous carbon supported Pt catalyst reported in literature. Moreover, chronoamerometry measurement performed in 1 M H_2SO_4 + 1 M CH_3OH at +0.7 V vs. Ag/AgCl. Sat KCl for 3 h shows the good stability.

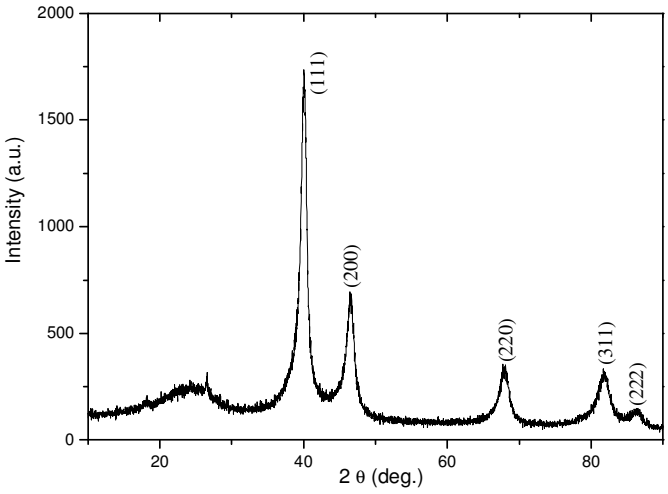

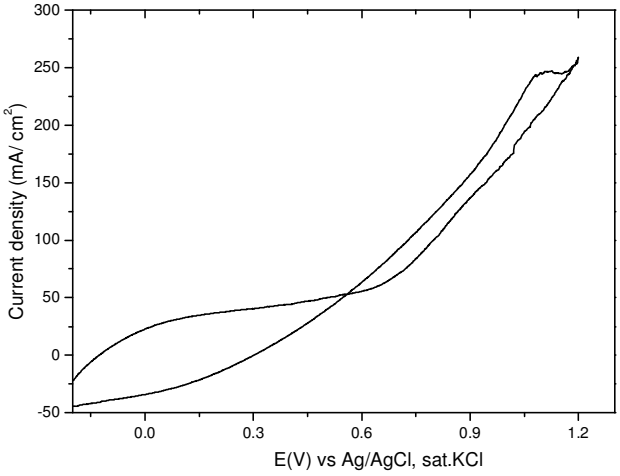

Figure 1. (Left) XRD pattern of 20 Pt/OMC (PVP).

Figure 2. (Right) CV of 20 Pt/OMC (PVP) catalyst recorded in 1 M H_2SO_4 and 1 M CH_3OH with scan rate 25 mV/s at 298 K.

1. D. Zhao, J. Feng, Q. Huo, N. Melosh, G. H. Fredrickson, B. F. Chemlka, G. D. Stucky, *Science.* **1998**, *279*, 548.
2. B. Viswanathan, *Catal. Today.* **2009**, *141*, 52.
3. J. Zeng, J. Y. Lee, *J. Power Sources.* **2005**, *140*, 268.
4. V. Raghuveer, A. Manthiram, *J. Electrochem. Soc.* **2005,** 152, A1504.

Synthesis of noble metal (Ag, Au, Pt and Pd) nanoparticles by oxalate-based methods

S. Navaladian

In recent times, nanomaterials are given much attention by researchers due to their advantages over bulk counterparts and due to the advancement in electron microscopic techniques. The physical and chemical properties of the nanomaterials are found to be different from that of the bulk counterparts. Not only the size but also the morphology of the nanomaterials is important due to the alteration in their properties with respect to the morphology. Hence, evolution of strategies for the synthesis of various materials with some specific morphology is required as various factors such as rate of the reaction, reaction condition, capping agent and solvent etc. have the influence on the resulting morphology of the materials. Noble metal nanoparticles exhibit potential applications in various fields such as environment, biomedicine, catalysis, optics and electronics. Hence, the present work deals with the synthesis of nanomaterials of silver, gold, platinum, palladium by oxalate-based mathods. Oxalate dianion was chosen as the reducing agent due to its good reducing capacity.

Since silver oxalate is a stable solid and it decomposes at 140 °C to yield metallic silver, its decomposition pathway has been chosen for the synthesis of Ag nanoparticles.

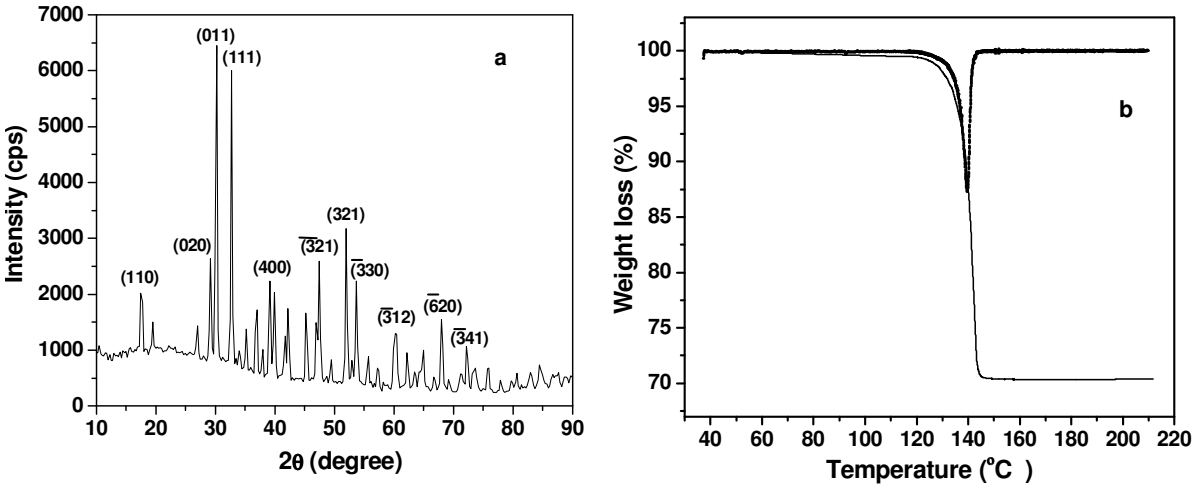

Figure 1. Powder XRD pattern (a) and TGA profile (b) of silver oxalate

Synthesis of Ag nanoparticles has been accomplished by (i) thermal, (ii) microwave (MW)-assisted and (iii) photochemical decomposition of silver oxalate in a

suitable medium using a capping agent. Methods of synthesis and morphological aspects of Ag nanoparticles are given in Table 1.

Method of synthesis	Capping agents and w/w ratio with $Ag_2C_2O_4$	Medium	Reaction time	Average particle size or range (nm)	Morphology of particles
Thermal	poly (vinyl alcohol) (PVA) 1:5	distilled water,	5 h	3 - 6	spherical
			3 h	2 - 4	spherical
		ethylene glycol	20 min	5 – 6	spherical
Microwave irradiation	poly (vinyl pyrrolidone) (PVP) 1:5	ethylene glycol	60 s	5 - 6	spherical
			75 s	15 - 45 (*b*) 20 -70 (*l*)	anisotropic
			90 s	50 -120	anisotropic
		diethylene glycol	75 s	15 -30	anisotropic
UV irradiation	poly (vinyl pyrrolidone) (PVP) 1:5	distilled water	10 min	1- 2	spherical particles
	CTAB 1:2			30	spherical
	CTAB 1:5			10 – 25 (*b*) 15 – 60 (*l*)	Rod+ spherical

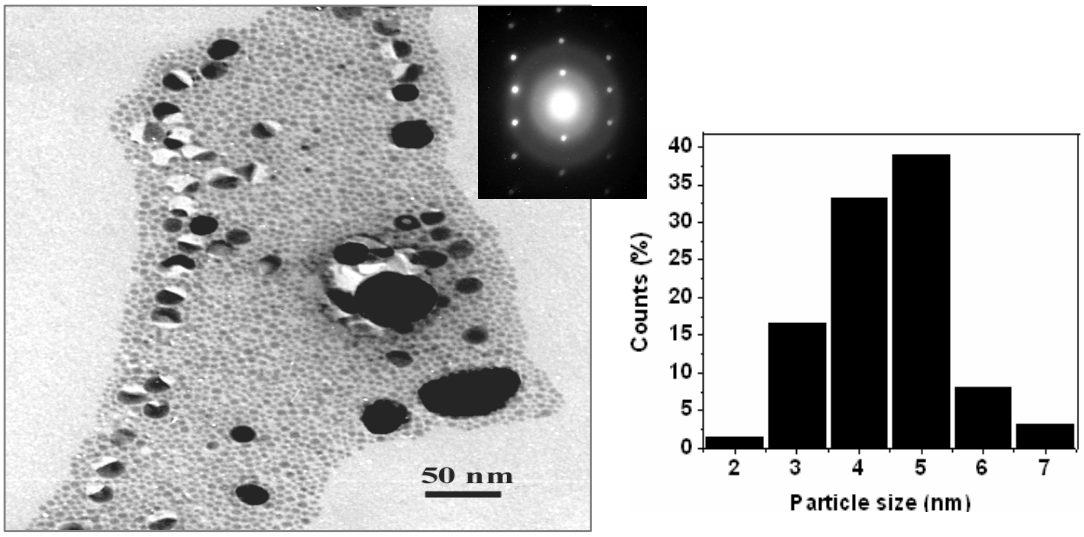

Figure 2. TEM images of Ag nanoparticles synthesized in water with $Ag_2C_2O_4$ to PVA weight ratio (a) 1:5 refluxing for 5h (SAED pattern is shown).

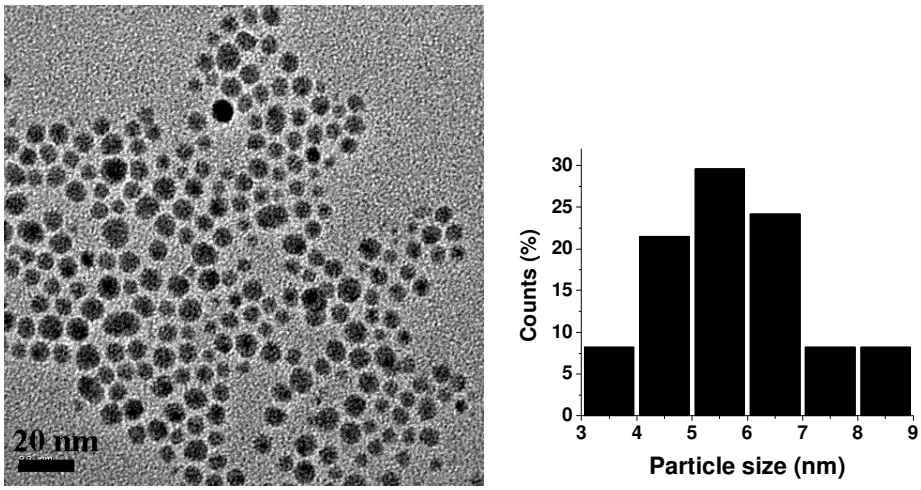

Fig. 3. HRTEM image and particle size distribution of Ag nanoparticles formed in ethylene glycol by the microwave exposure for 60 s.

Microwave -assisted method is more rapid than the other two methods. In the both cases, the chemical reduction by capping agents was observed. Ag nanoparticles synthesized by the thermal decomposition method was tested for antimicrobial activity against *E. Coli*. In the case of gold, reduction of Au(III) by oxalate in the presence of PVP at room temperature yields nanostructures like gold nanoplates and triangles as well as nanowires, depending upon the concentration of oxalate. In this case, kinetics of the reduction and particle growth have been monitored using UV-visible spectra during the

reaction for various ratios of reactants. Carbon supported Au nanowires and platinum catalysts have been attempted for the methanol electro-oxidation reaction. Similarly, Pt nanowires have also been synthesized by oxalate reduction, but the reduction has been found to be slower than that of gold. In addition, palladium nanoparticles were synthesized in a short period by UV irradiation method. The mechanism of particles growth is discussed.

References

1. V.V. Boldyrev, *Thermo. Chim. Acta.* **388**, (2002) 63.
2. S. Navaladian, B. Viswanathan, R.P.Viswanath and T.K.Varadarajan, *Nanoscale Research Letters*, **2** (2007) 44.
3. S. Navaladian, C. M. Janet, B. Viswanathan, T. K. Varadarajan and R. P. Viswanath, *Journal of Physical Chemistry C*, **111** (2007) 14150.
4. S. Navaladian, B. Viswanathan, T.K. Varadarajan and R.P. Viswanath, *Nanotechnology*, **19** (2008) 045603.
5. S. Navaladian**,** B. Viswanathan, T.K. Varadarajan and R.P. Viswanath, *Nanoscale Research Letters*, **4** (2009) 181.
6. S. Navaladian**,** B.Viswanathan, T.K. Varadarajan and R.P. Viswanath, *Nanoscale Research Letters*, **4** (2009) 471.

Terminal Oxidation of Dodecane using Microporous Alumino phosphate catalysts

M. Anil kumar, B. Viswanathan and P. Selvam

National Centre for Catalysis Research, Department of Chemistry,
Indian Institute of Technology Madras, Chennai 600 036

Linear alkanes are so notoriously difficult to oxidize that their very name – paraffins, from the Latin *parum affinis* (slight affinity)-emphasizes their inertness. n-Dodecane, for example, is not attacked by boiling nitric acid, concentrated sulphuric acid, potassium permanganate, or chromic acid. It is widely acknowledged that the controlled oxyfunctionalization of alkanes is one of the major challenges of modern catalysis; particularly desirable products (alcohols, ketones etc.,) are those that are oxidized at the terminal position, since these serve as feedstocks for the chemical and pharmaceutical industries. It is well known that some enzymes are capable of performing selective terminal oxidations without the necessary stability for use in the conditions employed for pure inorganic catalysts. Selective partial oxidations are easier to control when hydrogen peroxide or organic hydroperoxides are used as oxygen donors.

Thomas and co-workers succeeded in the preparation of pure inorganic catalysts that allows for the oxidation of n-alkanes at the terminal carbon atoms with high selectivity using molecular oxygen. These catalysts have the $AlPO_4$-18 (AEI) topology. These are eight-ring molecular sieves with pore openings formed by eight TO_4 tetrahedra (T=Al, P, Co, Mn) and a pore diameter of about 0.38 nm. With such catalysts it seems feasible that the terminal carbon atom of the reactants approaches the active sites and is oxidized at the end of the hydrocarbon chain to give the respective alcohols.

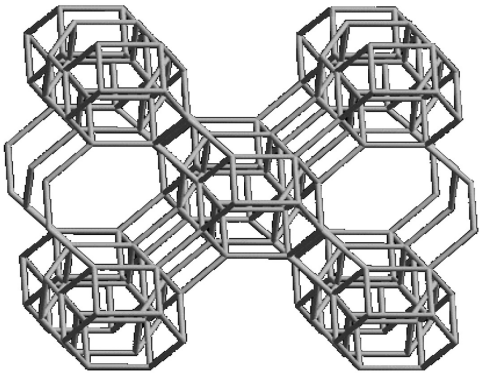

AEI

Choice of Catalysts:

We have selected the molecular sieve known as Metal substituted aluminophosphate (MeAlPO-18), which has pores similar to the Zeolites. A few atom percent of various divalent metal ions may be readily accommodated into this material's framework tetrahedral sites, as isomorphous replacements for Al (III) ions. This is done by template hydrothermal synthesis. The template is driven off completely by calcining in oxygen at ~550°C, during which process the redox ions (Co (II) or Mn (II)) are raised to their +3 oxidation states. During oxidation the transition metal ions return to their +2 states.

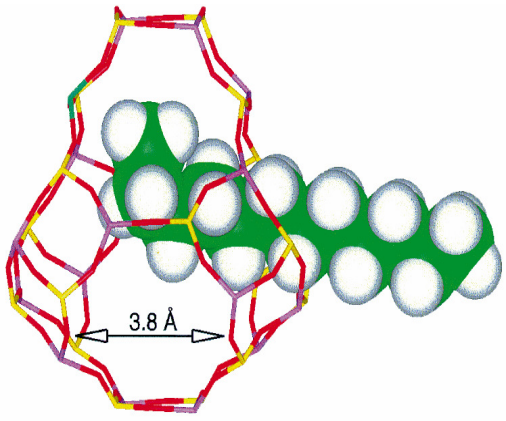

. AlPO-18 framework containing active centre (Mn (III) or Co (III)) at one end and Dodecane is entering into the framework through the pores.

Among various metal substituted AlPO-18 catalysts, Co-substituted analogues are shown to be effective catalysts for the reaction. Another class of AlPOs known as Cobalt substituted AlPO-34 catalysts also have been tried which are having a similar pore size as that of AlPO-18 catalysts.

Characterization:

XRD

CoAlPO-18

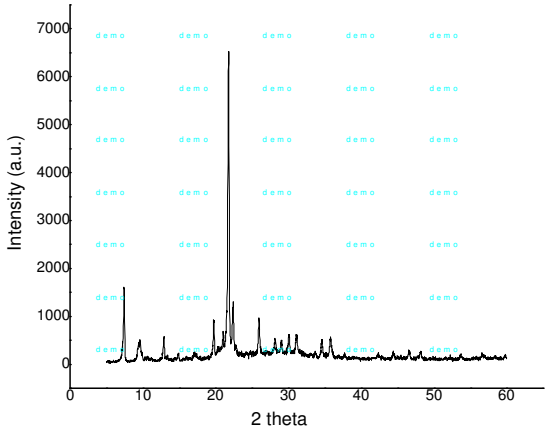

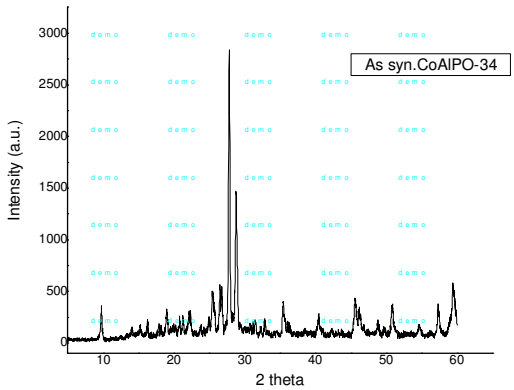

Reaction Conditions :
15 ml Dodecane, 0.5 g catalyst, 15 ml TBHP, 5 bar air, at 120°C and for 24 h.

Results:

With TBHP an oxidant CoAlPO-18 catalyst showed better conversion of dodecane compared to CoAlPO-34 catalyst. In addition to the desired 1-dodecanol, valuable products like 2-dodecanol, 3-dodecanon and some other products were also obtained.

References :

1. R. Raja, G. Sankar, and J.M.Thomas ; Angew. Chem. Int. Ed. 2000, 39, No.13
2. Yining Huang, Bryan A. Demko, and Christopher W. Kirby; *Chem. Mater.*, **2003**, 15 (12), 2437-2444

Hydroprocessing of diesel and vegetable oil blends

T.M. Sankaranarayanan*, M. Banu, A.K. Tiwari[a] and S. Sivasanker
National Centre for Catalysis Research, Indian Institute of Technology - Madras, Chennai-600036
[a] Summer Research Fellow (2009) from NIT, Tiruchirapalli

Introduction:

Fatty acid mono esters (FAME, biodiesel) are presently blended with desulfurized diesel in amounts ranging from 5 – 20% for use in transport vehicles. Biodiesel itself is manufactured in a separate process by the transesterification of vegetable oils with methanol mostly over alkali catalysts in which glycerol is obtained as a byproduct (up to about 10wt%). It needs to be transformed into value added chemicals to improve the economic viability of biodiesel.

In the present study, we report the direct hydroprocessing of blends of vegetable oil and straight run diesel at moderate pressures and temperatures. The main advantages of this process are the elimination of a separate transesterification step, the avoidance of by-product glycerol and increasing the energy content of the fuel.

Experimental:

Two diesel and vegetable oil blends (80:20 and 60:40 by wt, diesel:oil) were used in this study. The diesel was a straight run fraction (S, 1.76%) supplied by CPCL, Chennai and the vegetable oil was a commercial refined sunflower oil (cooking oil). The hydroprocessing of the blends was carried out at different process conditions in a high pressure fixed bed reactor using 30 g of catalyst. The process parameters were: temperature, 320 - 350°C, pressure, 30 – 60 bars, WHSV, 1 – 4 h^{-1} and H_2/oil ratio, 500v/v. A Ni-Mo-alumina catalyst was used in the study. To facilitate the conversion of the vegetable oil in the feed, an acidic component (zeolite beta supplied by Zeolyst) was incorporated in the catalyst formulation. The composition of the catalyst was NiO (12 wt%), CoO (3 wt%), beta (30wt%) and alumina (55wt%). The catalyst was presulfided with a DMDS/diesel feed (2 wt % S) prior to carrying out the catalytic studies. Product analysis was done in a GC using a short metal capillary column.

Results and discussion:

Product analysis revealed that the triglyceride molecules transformed mostly into C_{17} and C_{18} n-paraffins. At low severity conditions, small amounts of free fatty acids were also detected in the case of the 40% blend. Methane, propane, carbon dioxide and water were the other products from the vegetable oil. The formation of the different products from a hypothetical triglyceride molecule is shown in Figure 1. The conversion of the vegetable oil component and the relative amounts of the C_{17} and C_{18} paraffins (in the product from the vegetable oil component) at different process conditions are presented in Table 1. The vegetable oil transforms entirely into hydrocarbons in the case of the 20% blend at 320°C, 60 bar pressure and WHSV of $1h^{-1}$ (Table 1). However, at lower pressures and higher feed rates, the conversion of the vegetable oil is not complete. In the case of the 40% blend, oil conversion is less than 100% at most conditions used in

the study with small amounts of free fatty acids being detected at lower pressures (45 and 30 bars).

It is found that the relative amount of the C_{17} and C_{18} paraffins formed from the vegetable oil is dependent on the process conditions. The C_{17}/C_{18} hydrocarbon ratio appears to be dependent on both the fission mode (Fig. 1) and the relative conversion of the unconverted oxygenates (free fatty acids and alcohols) in the product. As the vegetable oil contained more C_{18} fatty acid components (95%) than C_{17} fatty acid components (5%), it appears that the a substantial amount of C_{17} paraffin found in the product is formed by cracking as shown in Fig. 1. Glycerol was not detected in any of the product samples. Traces of mono- and di-glycerides could also be identified in some products suggesting that the triglyceride molecule undergoes sequential cracking. Also, the fatty acids are probably the intermediates in the formation of a portion of the hydrocarbons

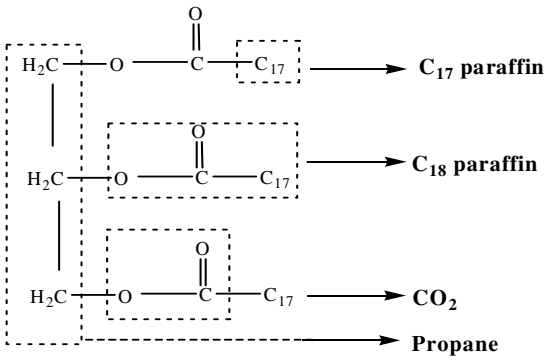

Fig. 1. The formation of the different products from a triglyceride molecule

Table 1. Hydroprocessing of diesel-vegetable oil blends at different conditions

Feed	Temp. (°C)	Pressure (bar)	WHSV (h^{-1})	Conv. of triglycerides (%)	% HDS	nC_{17}/nC_{18} (GC peak)
20%	320	60	1	100	64.7	0.300
blend	330	60	1	100	72.5	0.393
	340	60	1	100	86.1	0.556
	320	60	2	99.5	-	0.650
	320	45	2	99.0	-	0.746
	320	30	2	98.5	-	0.767
40%	320	60	2	92.0	60.0	0.620
blend	330	60	2	94.0	-	0.742
	340	60	2	95.0	-	0.767
	320	45	2	83.0	-	0.676
	320	30	2	79.0	-	0.786
Diesel	330	60	1	-	75.5	1.158

During the reaction, substantial hydrodesulfurization (HDS) of the feed also takes place. The percentage of S removed during the reaction is also presented in the above table. It appears that the presence of the vegetable oil (oxygenates) does not impede the desulfurization reaction.

Conclusion

The studies reveal that it is possible to transform diesel-vegetable oil blends at relatively moderate operating HDS conditions into a pure hydrocarbon fuel provided a suitable acidic hydrocracking component (such as zeolite beta) is incorporated in the catalyst. An advantage of the process is that it can also be used in the case of non-edible vegetable oils containing free fatty acids.

Acknowledgement: We thank CPCL, Chennai for the SR diesel and for S-analysis.